



Kent Academic Repository

Mao, Chun-Xu, Gao, Steven, Wang, Yi, Liu, Ying, Yang, Xue-Xia, Cheng, Zhiqun and Geng, Youlin (2018) *Integrated Dual-Band Filtering/Duplexing Antennas*. IEEE Access, 6 . ISSN 2169-3536.

Downloaded from

<https://kar.kent.ac.uk/66227/> The University of Kent's Academic Repository KAR

The version of record is available from

<https://doi.org/10.1109/ACCESS.2018.2805224>

This document version

Publisher pdf

DOI for this version

Licence for this version

CC BY (Attribution)

Additional information

Versions of research works

Versions of Record

If this version is the version of record, it is the same as the published version available on the publisher's web site. Cite as the published version.

Author Accepted Manuscripts

If this document is identified as the Author Accepted Manuscript it is the version after peer review but before type setting, copy editing or publisher branding. Cite as Surname, Initial. (Year) 'Title of article'. To be published in *Title of Journal*, Volume and issue numbers [peer-reviewed accepted version]. Available at: DOI or URL (Accessed: date).

Enquiries

If you have questions about this document contact ResearchSupport@kent.ac.uk. Please include the URL of the record in KAR. If you believe that your, or a third party's rights have been compromised through this document please see our [Take Down policy](https://www.kent.ac.uk/guides/kar-the-kent-academic-repository#policies) (available from <https://www.kent.ac.uk/guides/kar-the-kent-academic-repository#policies>).

Received December 30, 2017, accepted February 6, 2018, date of publication February 12, 2018, date of current version March 12, 2018.

Digital Object Identifier 10.1109/ACCESS.2018.2805224

Integrated Dual-Band Filtering/ Duplexing Antennas

CHUN-XU MAO¹, STEVEN GAO², (Senior Member, IEEE), YI WANG³, (Senior Member, IEEE),
YING LIU⁴, (Senior Member, IEEE), XUE-XIA YANG⁵, (Senior Member, IEEE),
ZHI-QUN CHENG⁶, AND YOU-LIN GENG⁶

¹School of Electrical Engineering and Computer Science, The Pennsylvania State University, PA 16801, USA

²School of Engineering and Digital Arts, University of Kent, Canterbury CT2 7NZ, U.K.

³Department of Electronic Electrical and Systems Engineering, University of Birmingham, Birmingham B15 2TT, U.K.

⁴National Laboratory of Science and Technology on Antennas and Microwaves, Xidian University, Xi'an 710071, China

⁵Shanghai Institute for Advanced Communication and Data Science, Shanghai University, Shanghai 200444, China

⁶School of Electronics and Information, Hangzhou Dianzi University, Hangzhou 310018, China

Corresponding author: Chunxu Mao (cm688@kent.ac.uk)

This work is supported by U.K. EPSRC under Grant EP/N032497/.

ABSTRACT In this paper, the state-of-the-art integrated filtering antennas with dual-band operation are first reviewed. Then, two designs of dual-band microstrip filtering antennas with a low-frequency ratio are presented. The 1st design is a dual-band dual-polarization (DBDP) antenna with a frequency ratio of 1.2 on a single patch, by employing the coupled resonator technique. Two bands at each polarization are achieved by vertically coupling a hairpin resonator with a patch through a slot in the ground plane and then coupled to a dual-mode stub loaded resonator. Each band exhibits a 2nd-order filtering performance with improved bandwidth and out-of-band rejection. Such an integration technique could significantly reduce the dimension and the complexity of the traditional DBDP antennas/arrays. In the 2nd design, a novel dual-port dual-band antenna (with a frequency ratio of 1.38) with the integrated filtering and duplexing functions is proposed. The frequency duplexing function is implemented by coupling a single patch with two sets of resonator-based filtering channels via a U-slot resonator inserted in the ground. This device seamlessly integrates the functions of duplexers, filters, and antennas in a very compact structure.

INDEX TERMS Antenna, dual-band, dual-polarized, duplexing antenna, filtering antenna.

I. INTRODUCTION

Radio frequency (RF) frontends with integrated multiple functions have attracted wide attention in the recent years due to many advantages over the traditional cascaded RF frontends. By merging multiple functions such as radiation, filtering, power-splitting and/or duplexing into one device, a reduced component number and significant compact circuit footprint can be realized without the traditional transmission line and interfaces between them [1]–[4]. The other important virtue of the integrated design is the enhanced performance. For example, by exploiting the electromagnetic couplings, the bandwidth, frequency selectivity, and out-of-band rejection can be increased [5]–[10]. Additionally, the integration design could augment functionalities. For example, a duplexer and an antenna can be combined to realize a new dual-port duplexing antenna [11], [12]. The integration of RF frontends could also contribute to the reduction of the loss and cost of mm-wave devices [13]–[16].

The dual/multi-band operation with polarization diversity are in high demand in the current and next generation wireless systems for catering different wireless applications [17]–[19]. The dual-band antennas with different I/O ports are also preferable in many practical applications. Most of the integrated designs work at a single band and polarization. In [20]–[26], integrated filtering antennas with dual-band operation were reported. However, due to the asymmetrical structure of the radiation elements, most of them are not suitable for dual-polarization applications. In [23], a dual-band dual-polarization (DBDP) filtering array antenna was achieved by coupling a dual-mode resonator to two nested patches. However, the restriction on the sizes of the nested elements makes this design unsuitable for low frequency-ratio (less than 1.5) applications.

In this paper, two novel integrated dual-band filtering antennas with a low frequency ratio are proposed. Both designs make use of the strong couplings between the

resonant structures to generate two closely situated operation bands. In the first design, a DBDP filtering antenna element with a low frequency-ratio of 1.2 is achieved using a single square patch. In the second design, a dual-port dual-band antenna with integrated duplexing and filtering functions is developed.

This paper is organized as follows. Section II reviews of the state-of-the-art dual-band filtering antennas. Section III proposes a low frequency-ratio DBDP filtering antenna. Section IV presents the second design of the dual-port duplexing filtering antenna, followed by a conclusion in Section V.

II. REVIEW OF DUAL-BAND FILTERING ANTENNAS

This section firstly reviews the recently reported dual-band filtering antennas categorized by their design techniques. The advantages and disadvantages of each design are discussed.

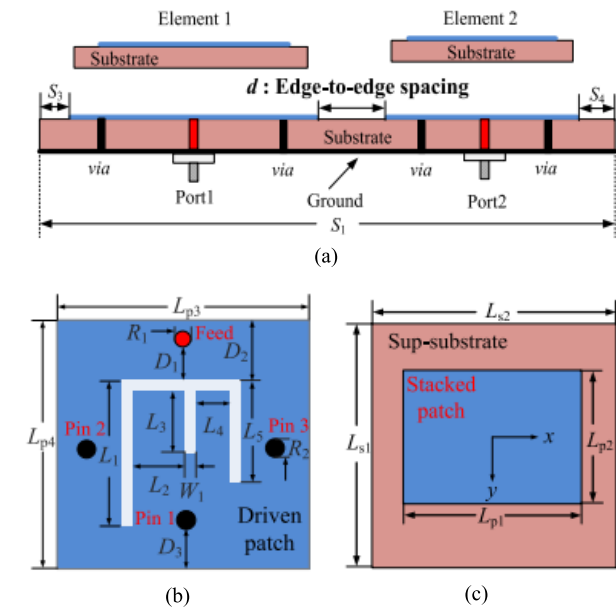


FIGURE 1. Configuration of the dual-band filtering antenna in [22]: (a) side view, (b) driven patch, and (c) parasitic patch.

A. LATERALLY PLACED DUAL-BAND FILTERING ANTENNA

By placing two single-band filtering antennas close to each other and side-by-side, dual-band antennas with excellent frequency selectivity and a high isolation between the two closed antennas can be achieved. Fig. 1 shows such a design reported in [22]. The two antenna elements have similar configuration, which consists of a parasitic patch, a driven patch with inserted shorted pins and slots and a ground plane. The stacked parasitic patch was used to broaden the bandwidth of the antenna and introduce a radiation null at the high-band. The slots and the shorted pins are employed here to generate other radiation nulls at the low-band. Therefore, very good frequency selectivity and isolation between the two antennas can be realized. This physically separated antennas could also render the flexibility to control and optimize the two bands.

However, this also leads to a large circuit footprint due to the two separate sets of radiators and feeding networks.

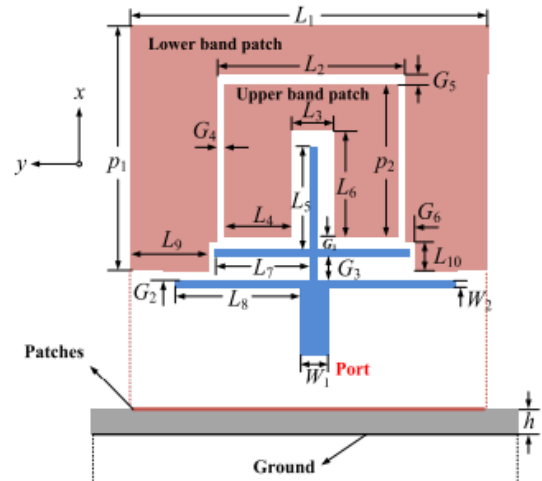


FIGURE 2. Configuration of the aperture-shared dual-band filtering antenna in [24].

B. APERTURE-SHARED DUAL-BAND FILTERING ANTENNA

To make the dual-band filtering antenna more compact, one method is to embed the smaller high-band radiator inside the low-band radiator, sharing the same aperture [23]–[24]. Fig. 2 shows the configuration of a compact aperture-shared dual-band filtering antenna reported in [24]. The antenna consists of two nested U-shaped patches work at different operation bands. They are fed by a multi-stub microstrip line. The two resonances of the microstrip lines are tuned to match with the resonant frequencies of the two patches, producing two operation bands each with a 2nd-order filtering characteristic.

The antenna has an evident advantage of compact size due to the two radiators are embedded and printed on the same layer. In addition, two radiation nulls were generated outside of the both bands, shaping the sharp roll-offs. However, the layout of the two radiators in this design constrains its ability to control the frequency ratio of the two bands. Besides, the asymmetrical configurations of the radiators prevent its use in dual-polarization applications.

C. RADIATOR-SHARED DUAL-BAND FILTERING ANTENNA

For further integration and miniaturization, different resonant modes of a patch can be used to design the dual-band operation. In [25] and [26], two resonant modes of a patch were generated by inserting a U-shaped slot in the patch. The two resonant modes can be controlled by adjusting the dimensions of the patch and the slot line, respectively. Fig. 3 shows a design of a radiator-shared dual-band filtering antenna in [26]. The two resonant modes of the U-slot patch are separately coupled with a stub-loaded resonator (SLR), resulting in the dual-band operations and each with a 2nd-order filtering performance.

Since the two resonant frequencies of the U-slot patch and the SLR can be independently controlled, good flexibility

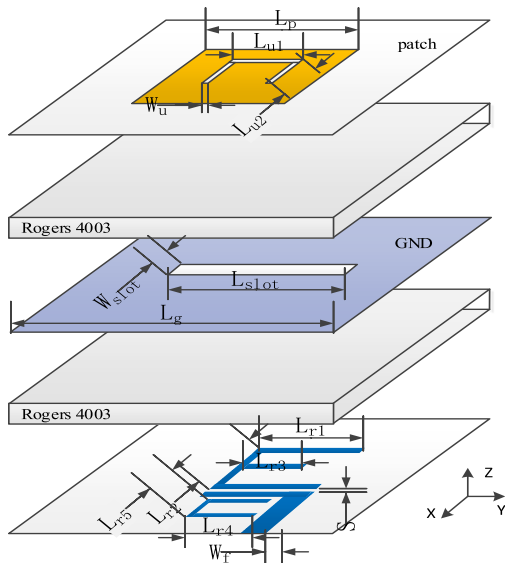
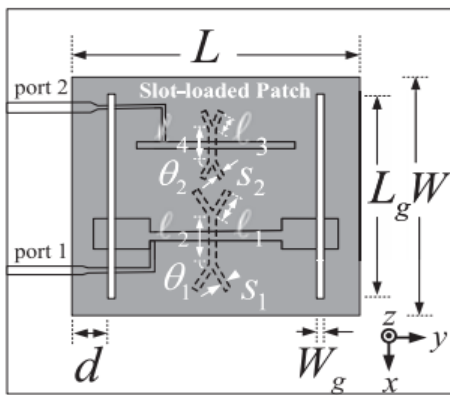
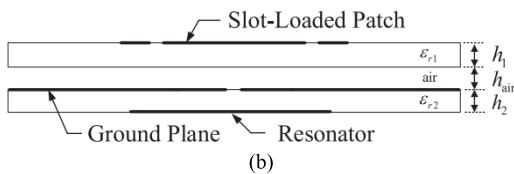


FIGURE 3. Configuration of the dual-band filtering antenna with shared radiator in [26].



(a)



(b)

FIGURE 4. Configuration of the dual-port dual-band filtering antenna in [27]: (a) top view, (b) side view.

in adjusting the frequency ratio of the two bands can be achieved. An added advantage is that the higher order modes of the SLR and the U-slot patch are mismatched with each other, resulting in the cancellation of the high-order modes and therefore the wideband harmonic suppression. However, the lack of rotational symmetry of the U-slot patch limits its applications in dual-polarization antennas.

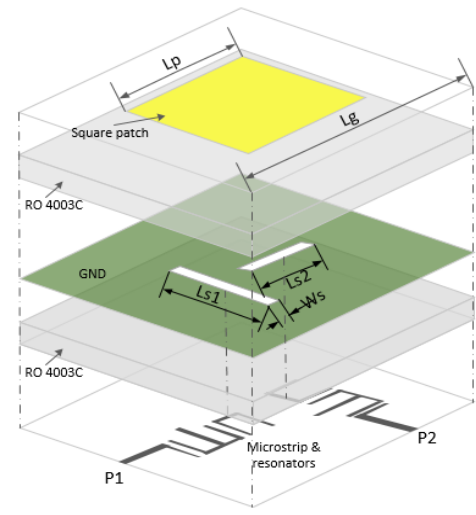
D. RADIATOR-SHARED DUPLEXING FILTERING ANTENNA

In [27], a dual-band filtering antenna with two separate ports work at different frequency bands was investigated and is shown in Fig. 4. This design integrated the duplexing and

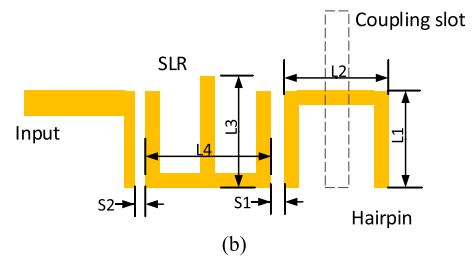
radiation functions in a single device. The antenna uses the TM10 and TM30 modes for achieving the broadside radiation. By inserting two parallel slots in the patch, the two modes are coupled with the feeding networks/resonators, respectively, generating two frequency duplexing bands. However, due to the high-order mode are used in the design, it is difficult to achieve a low frequency ratio. Other limitations in the performance include the relatively low frequency selectivity and low isolation between the two ports (20 dB).

III. DESIGN-1: SINGLE-PATCH DUAL-BAND DUAL-POLARIZED FILTERING ANTENNA

To overcome the limitations of the dual-band dual-polarized filtering antennas described in Section-II, a novel DBDP filtering antenna with a low frequency ratio using a single square patch is proposed here.



(a)



(b)

FIGURE 5. Configuration of the proposed low frequency-ratio DBDP filtering antenna (Antenna-I): (a) exploded view; (b) feeding resonators of each polarization. Lp = 17.8 mm, Lg = 50 mm, Ls1 = 11.8 mm, Ls2 = 10.3 mm, Ws = 0.9 mm, L1 = 5.8 mm, L2 = 4 mm, L3 = 7 mm, L4 = 6.5 mm, S1 = 1.2 mm, S2 = 0.3 mm.

A. CONFIGURATION

Fig. 5(a) shows the configuration of the proposed low frequency-ratio DBDP filtering antenna, denoted as Antenna-I. The square patch is printed on the top layer of the upper substrate, whereas the feeding networks are printed on the bottom layer of the lower substrate. The patch and feeding structures share the same ground plane in the middle layer.

In the ground plane, two slots are perpendicularly placed to excite the orthogonal polarizations of the patch. Fig. 5(b) shows the feeding network for each polarization, which consists of a hairpin resonator and an SLR. The patch is first coupled to the hairpin resonator, which is then coupled to the SLR. The patch and the hairpin resonator are served as the single-mode resonators. The SLR is a dual-mode resonator, which can be analyzed using the odd- and even-mode methods [28]. The optimizations were performed using High Frequency Structural Simulator (HFSS) and the optimized dimensions are presented in the caption of Fig. 5.

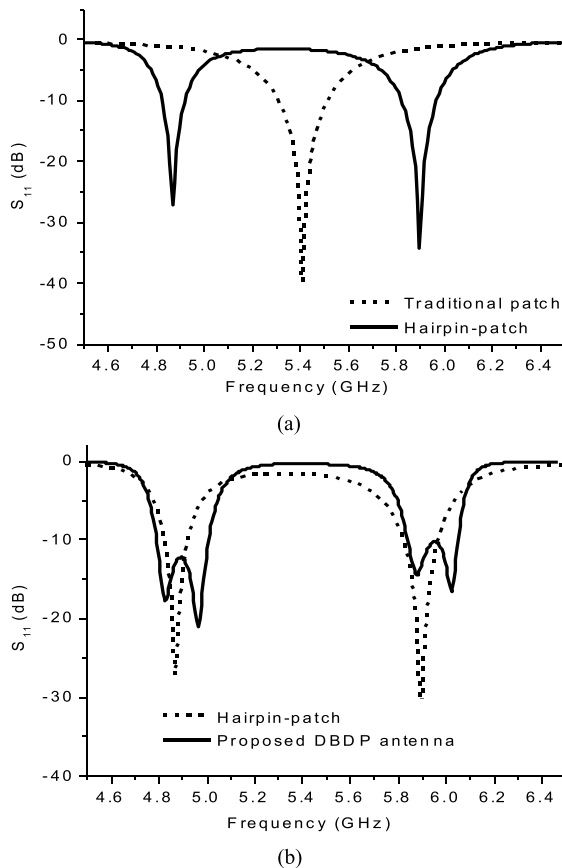


FIGURE 6. Comparison of the simulated S_{11} of the antennas: (a) between a traditional microstrip-fed patch and the hairpin-fed patch, (b) the hairpin-fed patch antenna with and without the cascaded SLR.

B. OPERATION PRINCIPLE

One major technical contribution of this work is that the DBDP characteristics are realized on a single patch. The design principle of this antenna is explained as follows. First, the patch and the hairpin resonator are tuned to have the same resonant frequency ($f_0 = 5.4$ GHz) and coupled through the slot in the ground. By increasing the coupling intensity, the coupled hairpin-patch generates two split resonant frequencies ($f_1 = 4.9$ GHz and $f_2 = 5.9$ GHz), as shown in Fig. 6(a) in comparison with a traditional microstrip-fed patch antenna. These two resonances define the two operation bands. The two frequencies can be adjusted by changing

the length of the coupling aperture, L_{s1} and the frequency ratio of the two bands can be achieved as required. The hairpin resonator is then coupled to the dual-mode SLR, which is tuned to match the resonant frequencies of the hairpin-patch. This results in the 2nd-order filtering response for each band, as shown in Fig. 6(b). Similarly, dual-band filtering characteristics can be achieved for the other polarization.

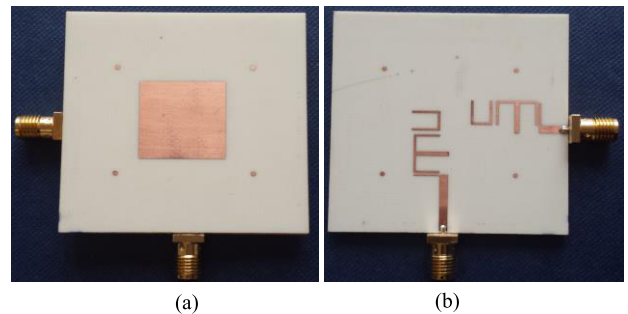


FIGURE 7. Prototype of the low frequency-ratio DBDP filtering antenna (Antenna-I): (a) front view, (b) back view.

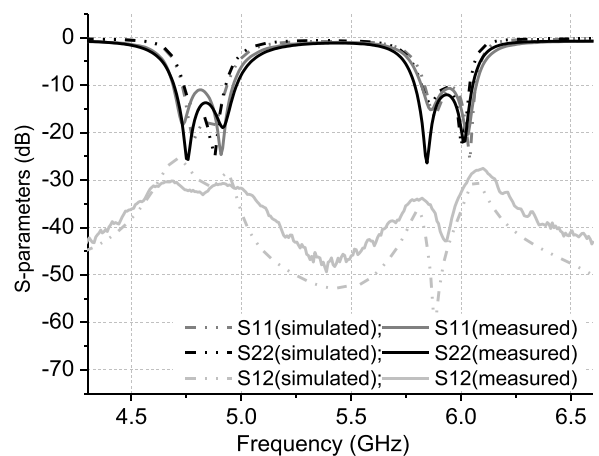


FIGURE 8. Simulated and measured S-parameters of Antenna-I.

C. RESULTS AND DISCUSSION

The proposed DBDP filtering antenna (Antenna-I) was prototyped and measured. Fig. 7 shows the front- and back-view of the prototype. Fig. 8 presents the measured and simulated S-parameters. The measurements agree well with the simulations, showing two operation bands from 4.75 to 4.98 GHz (FBW = 4.8%) and 5.75 to 6.05 GHz (FBW = 5.1%) for each port/polarization. The achieved frequency ratio is 1.22. The antenna also exhibits the 2nd-order filtering performance with two reflection zeros observed in both bands. In addition, the antenna demonstrates the high isolation with the measured $|S_{12}|$ below to -30 dB at both bands. It should be noted that two transmission nulls are produced at around 4.8 and 5.85 GHz. These nulls are produced by purposely conceiving the cross-coupling between the resonators, which is beneficial to enhancing the isolation between the

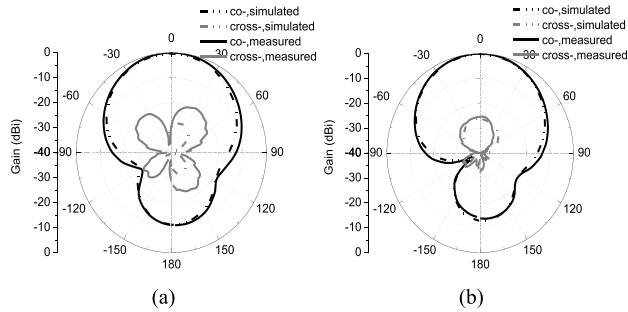


FIGURE 9. Simulated and measured normalized radiation patterns of the DBDP antenna at 4.85 GHz: (a) P1 is excited, (b) P2 is excited.

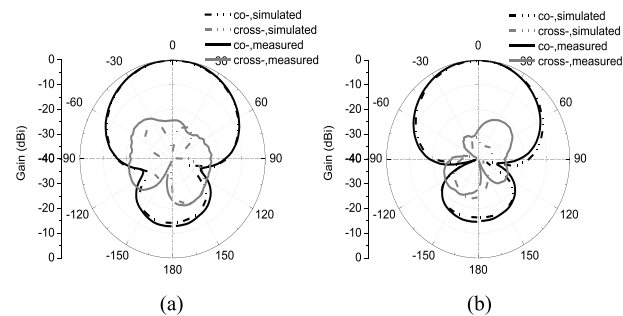


FIGURE 10. Simulated and measured normalized radiation patterns of the DBDP antenna at 5.85 GHz: (a) P1 is excited, (b) P2 is excited.

two polarizations. The minor discrepancies are attributed to fabrication and assembly tolerance.

Fig. 9 shows the simulated and measured normalized E-plane radiation patterns of the proposed DBDP antenna at 4.85 GHz. The measured results agree well with the simulations. The antenna exhibits consistent radiation patterns with the maximum radiation in the broadside direction when the two ports/polarizations are excited, respectively. The antenna also exhibits excellent polarization purity with the cross-polarization discrimination (XPD) higher than 28 dB (25 dB) for the X-polarization (Y-polarization). Fig. 10 shows the simulated and measured normalized radiation patterns of the high-band (5.85 GHz). Good agreement between the measurements and simulations is achieved when the antenna works at both polarizations. The measured XPD is higher than 25 dB.

Fig. 11 shows the simulated and measured realized gains of the DBDP filtering antenna. The measured result agrees reasonably well with the simulation, showing a gain of 7.2 dBi from 4.87 to 5.03 GHz and a gain of 7.5 dBi from 5.8 to 6.05 GHz, respectively. The gains drop noticeably out of the two bands, demonstrating a good filtering performance.

IV. DESIGN-2: DUAL-PORT DUPLEXING FILTERING ANTENNA

This section demonstrates the implementation of a novel dual-port dual-band antenna with a duplexing function. In this work, the two ports of the antenna are highly isolated and working at different frequency bands.

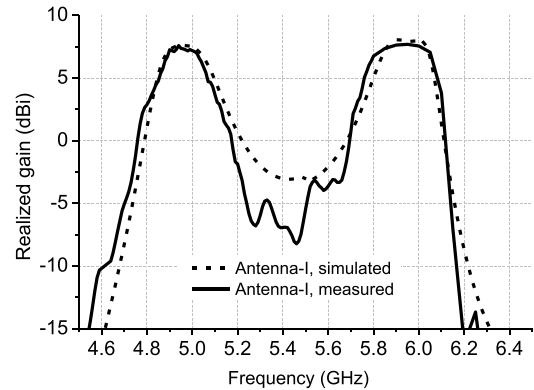


FIGURE 11. Simulated and measured realized gains of the DBDP filtering antenna.

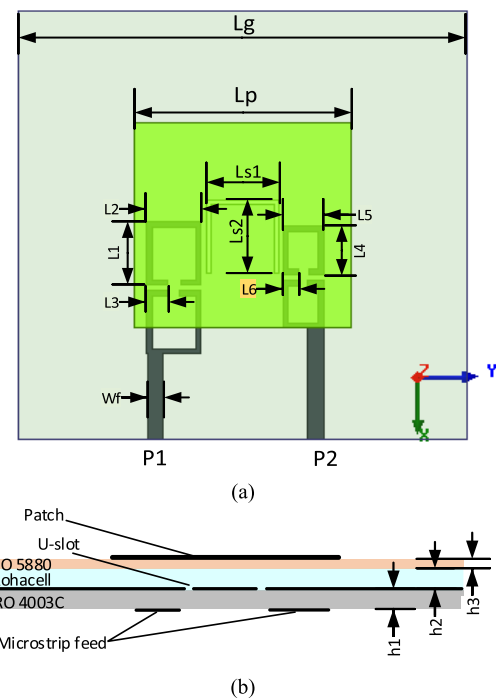


FIGURE 12. Configurations of the dual-port dual-band duplexing filtering antenna (Antenna-II). $L_g = 50$ mm, $L_p = 24$ mm, $W_f = 1.8$ mm, $L_1 = 7.5$ mm, $L_2 = 5.8$ mm, $L_3 = 1.55$ mm, $L_4 = 5.8$ mm, $L_5 = 4.3$ mm, $L_6 = 1.3$ mm, $L_{s1} = 8$ mm, $L_{s2} = 8.2$ mm, $h_1 = 0.8$ mm, $h_2 = 1$ mm, $h_3 = 0.254$ mm.

A. CONFIGURATION AND TOPOLOGY

Fig. 12 shows the configuration of the proposed dual-port duplexing filtering antenna (denoted as Antenna-II), which consists of two substrates and a 1 mm thick foam between them. The radiator is a square patch printed on the top layer of the upper substrate. The ground plane with an inserted U-shaped slot line is printed on the top layer of the lower substrate. The microstrip lines and resonators are printed on the bottom of the lower substrate. There are totally two ports and two groups of open loop resonators (half-wavelength resonator) as the filtering channels working at $f_1 = 4.3$ GHz and $f_2 = 6$ GHz, respectively.

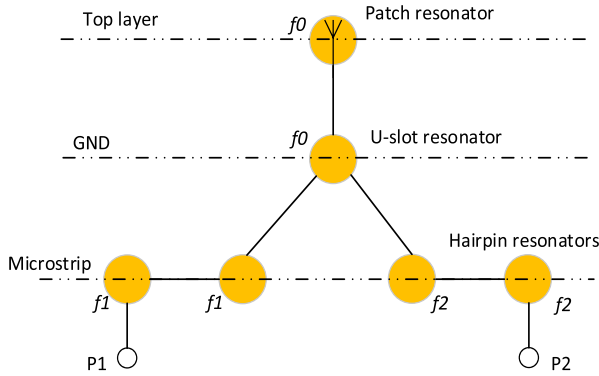


FIGURE 13. Topology of the dual-port dual-band duplexing antenna.

To illustrate the design mechanism, the dual-port duplexing antenna is modelled using a coupled-resonator topology, as shown in Fig. 13. The circles represent single-mode resonators and the solid lines represent the coupling between them. The patch resonator not only serves as the radiating element but also a single-mode resonator with the resonance of f_0 . The inserted U-slot resonator is adjusted to synchronously tune with the patch and the resonant frequency f_0 is split into two resonant frequencies f_1 and f_2 . These frequencies are then respectively coupled to the two groups of resonator-based filtering networks, generating two channels. Each of them has the 3rd-order filtering response.

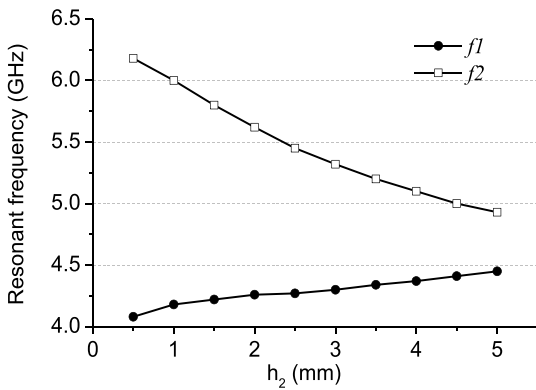


FIGURE 14. Resonant frequencies f_1 and f_2 with different h_2 .

In this design, the two resonant frequencies, as well as the frequency ratio, can be controlled by adjusting the coupling strength between the patch and the U-slot resonator. Fig. 14 shows the extracted resonant frequencies f_1 and f_2 as a function of the thickness of the foam, denoted as h_2 in Fig. 12. It is observed that the f_1 increases and f_2 decreases when the thickness of the foam increases. This reversed tendency provides the freedom to design the frequency ratio of the two operation bands. It is shown that the frequency ratio can be reduced to 1.1 when h_2 increases to 5 mm. As a demonstration, $h_2 = 1$ mm was chosen in this work for a frequency ratio of 1.38.

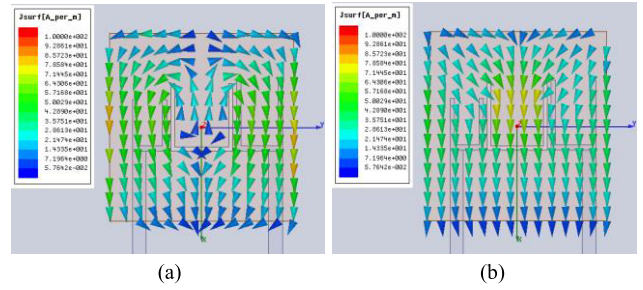


FIGURE 15. Simulated current distribution on the patch: (a) Port 1 is excited, at 4.3 GHz, (b) Port 2 is excited, at 5.9 GHz.

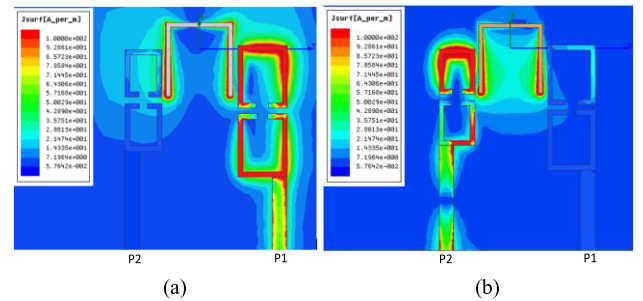


FIGURE 16. Simulated current distribution of the duplexing antenna on the feed and ground: (a) Port 1 is excited, at 4.3 GHz, (b) Port 2 is excited, at 5.9 GHz.

B. CURRENT DISTRIBUTION

Fig. 15 shows the simulated current distribution of the dual-band duplexing antenna. When Port 1 is excited (4.3 GHz), the current on the patch is bent and flows along an extended path. This enables the radiation at a lower band than the patch’s intrinsic resonance. When Port 2 is excited (5.9 GHz), however, the current on the patch is quite straight with a shorter path. Although the current distributions at both bands are slightly different, the antenna works in a quasi-TM10 mode in both cases, which results in the similar radiation in the broadside direction. The current distribution also predicts that the antenna has the consistent polarization characteristics at the two bands.

Fig. 16 shows the current distribution of the dual-port dual-band duplexing antenna on the feeds and ground plane. When antenna works at 4.3 GHz (Port 1 is excited), as can be seen from Fig. 16(a), strong current flows along the larger hairpin resonators and U-shaped slot. The current is significantly subdued on the feed of the high-band channel. In contrast, when the antenna works at 5.9 GHz (Port 2 is excited), the current mainly distributes on the smaller resonators and the common U-slot. The current on the channel of the low-band is very weak. This current distribution demonstrates that a very good isolation is achieved between the two channels/ports.

C. RESULTS AND DISCUSSION

The proposed dual-port dual-band duplexing filtering antenna was prototyped and measured to verify the design concept. Fig. 17 shows the front and back views of the Antenna-II.

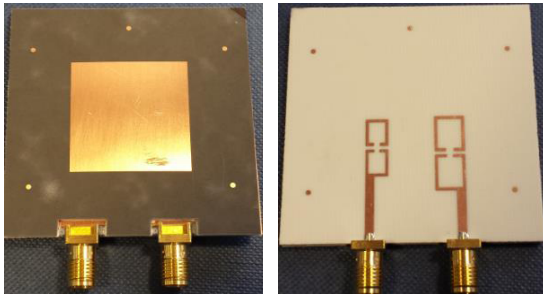


FIGURE 17. The front and back view of the dual-port dual-band duplexing antenna prototype.

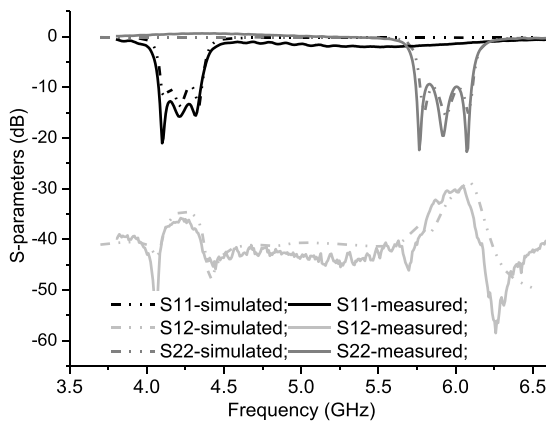


FIGURE 18. Simulated and measured S-parameters of the proposed duplexing antenna.

The simulated and measured S-parameters are presented in Fig. 18. A very good agreement between the measurements and simulations is achieved. When Port 1 is excited, a frequency band is achieved from 4.1 to 4.35 GHz (FBW = 5.9%). When port 2 is excited, a band from 5.8 to 6.15 GHz is achieved (FBW = 5.8%). At each band, the antenna exhibits the 3rd-order filtering characteristics with three reflection zeros observed. The antenna also shows excellent frequency selectivity and out-of-band rejection performance. The isolation between the two channels/ports is higher than 30 dB at both bands. As the frequency ratio reduces, the isolation between the two channels is deteriorated correspondingly.

Fig. 19 presents the simulated and measured realized gains of the Antenna-II when the two ports are excited, respectively. When Port 1 is excited, the antenna has a flat gain response of around 6.5 dBi in the lower band. In the higher band, the antenna achieves a flat gain of about 7 dBi when Port 2 is excited. The gains are noticeably reduced by more than 20 dB as the frequency shifts from the two operation bands, exhibiting an excellent filtering performance. The minor discrepancy is attributed to the measurement tolerance.

Fig. 20 shows the simulated and measured normalized radiation patterns of the dual-port dual-band duplexing antenna at 4.3 GHz when Port 1 is excited. The measurements and

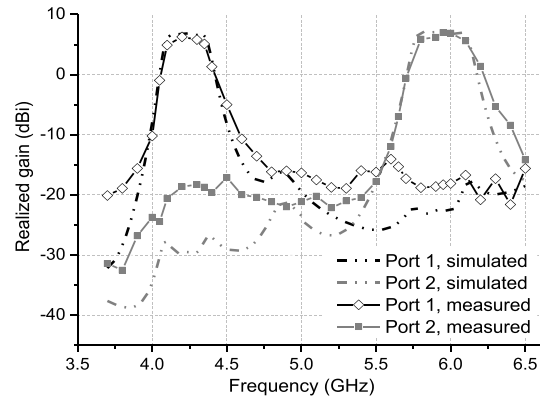


FIGURE 19. Simulated and measured gains of the proposed duplexing antenna.

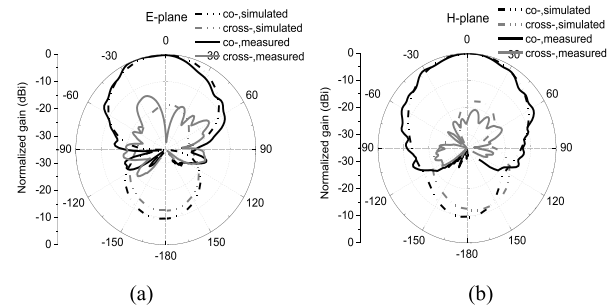


FIGURE 20. Simulated and measured normalized radiation patterns of the dual-port duplexing antenna at 4.3 GHz when Port 1 is excited: (a) $\varphi = 0^\circ$, (b) $\varphi = 90^\circ$.

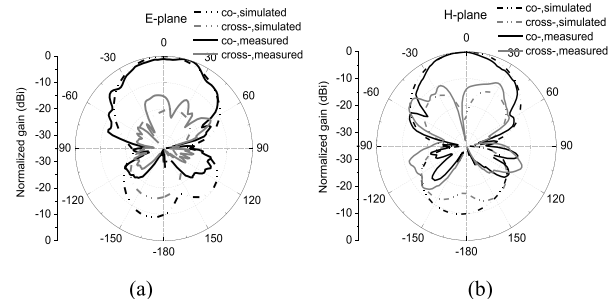


FIGURE 21. Simulated and measured normalized radiation patterns of the dual-port duplexing antenna at 5.9 GHz when Port 1 is excited: (a) $\varphi = 0^\circ$, (b) $\varphi = 90^\circ$.

simulations agree reasonably well with each other, showing the maximum radiation in the broadside direction. The measured cross polarization discrimination (XPD) is over 25 dB in both $\varphi = 0^\circ$ (E-plane) and $\varphi = 90^\circ$ (H-plane).

Fig. 21 shows the simulated and measured normalized radiation patterns of the antenna at 5.9 GHz when port 2 is excited. Similarly, the antenna exhibits the broadside radiation patterns in both $\varphi = 0^\circ$ and 90° planes. The measured XPD is over 15 dB in the broadside direction. The discrepancy between the simulations and measurements, especially the backward radiation, is caused by the blockage of the measurement instruments.

TABLE 1. Comparison With Other Dual-Band Filtering Antennas.

| Antennas | Number of Radiators | Isolation (dB) | Frequency Ratio | Dual-Polarization |
|----------|---------------------|----------------|-----------------|-------------------|
| [24] | 2 | 30 | 1.37 | No |
| [26] | 1 | - | 1.44 | No |
| [27] | 1 | 20 | 2.16 | No |
| Design-1 | 1 | 28 | 1.22 | Yes |
| Design-2 | 1 | 30 | 1.38 | No |

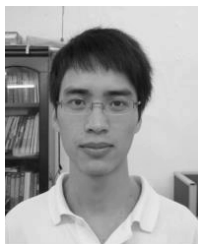
Table I compares the proposed two filtering antennas with other reported dual-band filtering antennas in [24], [26], and [27]. The first design (Design-1) can realize the dual-polarization characteristics at two operation bands using a single radiator. The frequency ratio is 1.22. Compared with [27], Antenna-II has a lower frequency ratio (1.38 versus 2.16), a higher frequency selectivity (3rd-order versus 2nd-order) and better duplexing performance/isolation (30 dB vs 20 dB). Although only single linear polarization is demonstrated in Antenna-II, it is possible to be developed to a dual-polarization antenna due to the symmetry of the square patch.

V. CONCLUSION

In this paper, two novel highly integrated dual-band filtering antennas with a low frequency-ratio are presented. The concept and design mechanism are discussed. In the first design, the dual-band dual-polarization characteristics with a frequency ratio of 1.2 are achieved using a single square patch. In the second design, a dual-port dual-band filtering antenna with integrated duplexing functions is proposed. The demonstrated integration technique is helpful in removing the separate bandpass filters and duplexers, and thus it could be potentially used in an integrated RF frontend with reduced volume, complexity and cost.

REFERENCES

- [1] C.-T. Chuang and S.-J. Chung, "A compact printed filtering antenna using a ground-intruded coupled line resonator," *IEEE Trans. Antennas Propag.*, vol. 59, no. 10, pp. 3630–3637, Oct. 2011.
- [2] C.-T. Chuang and S.-J. Chung, "Synthesis and design of a new printed filtering antenna," *IEEE Trans. Antennas Propag.*, vol. 59, no. 3, pp. 1036–1042, Mar. 2011.
- [3] O. A. Nova, J. C. Bohorquez, N. M. Pena, G. E. Bridges, L. Shafai, and C. Shafai, "Filter-antenna module using substrate integrated waveguide cavities," *IEEE Antennas Wireless Propag. Lett.*, vol. 10, pp. 59–62, 2011.
- [4] Z. H. Jiang and D. H. Werner, "A compact, wideband circularly polarized co-designed filtering antenna and its application for wearable devices with low SAR," *IEEE Trans. Antennas Propag.*, vol. 63, no. 9, pp. 3808–3818, Sep. 2015.
- [5] Y. Yusuf, H. Cheng, and X. Gong, "A seamless integration of 3-D vertical filters with highly efficient slot antennas," *IEEE Trans. Antennas Propag.*, vol. 59, no. 11, pp. 4016–4022, Nov. 2011.
- [6] C.-X. Mao, S. Gao, Y. Wang, F. Qin, and Q.-X. Chu, "Multi-mode resonator-fed dual polarized antenna array with enhanced bandwidth and selectivity," *IEEE Trans. Antennas Propag.*, vol. 63, no. 19, pp. 5492–5499, Oct. 2015.
- [7] C.-X. Mao et al., "An integrated filtering antenna array with high selectivity and harmonics suppression," *IEEE Trans. Microw. Theory Techn.*, vol. 64, no. 6, pp. 1798–1805, Jun. 2016.
- [8] P. F. Hu, Y. M. Pan, X. Y. Zhang, and S. Y. Zheng, "A compact filtering dielectric resonator antenna with wide bandwidth and high gain," *IEEE Trans. Antennas Propag.*, vol. 64, no. 8, pp. 3645–3651, Aug. 2016.
- [9] P. F. Hu, Y. M. Pan, X. Y. Zhang, and S. Y. Zheng, "Broadband filtering dielectric resonator antenna with wide stopband," *IEEE Trans. Antennas Propag.*, vol. 65, no. 4, pp. 2079–2084, Apr. 2017.
- [10] W. Duan, X. Y. Zhang, Y.-M. Pan, J.-X. Xu, and Q. Xue, "Dual-polarized filtering antenna with high selectivity and low cross polarization," *IEEE Trans. Antennas Propag.*, vol. 64, no. 10, pp. 4188–4196, Oct. 2016.
- [11] X.-J. Lin, Z.-M. Xie, P.-S. Zhang, and Y. Zhang, "A broadband filtering duplex patch antenna with high isolation," *IEEE Antennas Wireless Propag. Lett.*, vol. 16, pp. 1937–1940, 2017.
- [12] C. X. Mao, S. Gao, Y. Wang, F. Qin, and Q. X. Chu, "Compact highly integrated planar duplex antenna for wireless communications," *IEEE Trans. Microw. Theory Techn.*, vol. 64, no. 7, pp. 2006–2013, Jul. 2016.
- [13] H. Chu, C. Jin, J.-X. Chen, and Y.-X. Guo, "A 3-D millimeter-wave filtering antenna with high selectivity and low cross-polarization," *IEEE Trans. Antennas Propag.*, vol. 63, no. 5, pp. 2375–2380, May 2015.
- [14] Y. Yusuf and X. Gong, "Compact low-loss integration of high-Q 3-D filters with highly efficient antennas," *IEEE Trans. Microw. Theory Techn.*, vol. 59, no. 4, pp. 857–865, Apr. 2011.
- [15] H. Chu, J.-X. Chen, S. Luo, and Y.-X. Guo, "A millimeter-wave filtering monopulse antenna array based on substrate integrated waveguide technology," *IEEE Trans. Antennas Propag.*, vol. 64, no. 1, pp. 316–321, Jan. 2016.
- [16] H. Chu and Y.-X. Guo, "A novel approach for millimeter-wave dielectric resonator antenna array designs by using the substrate integrated technology," *IEEE Trans. Antennas Propag.*, vol. 65, no. 2, pp. 909–914, Feb. 2017.
- [17] S. Gao and A. Sambell, "Low-cost dual-polarized printed array with broad bandwidth," *IEEE Trans. Antennas Propag.*, vol. 52, no. 12, pp. 3394–3397, Dec. 2004.
- [18] S.-C. Gao, L.-W. Li, M.-S. Leong, and T.-S. Yeo, "Dual-polarized slot-coupled planar antenna with wide bandwidth," *IEEE Trans. Antennas Propag.*, vol. 51, no. 3, pp. 441–448, Mar. 2003.
- [19] S. Gao, L. W. Li, M. S. Leong, and T. S. Yeo, "A broad-band dual-polarized microstrip patch antenna with aperture coupling," *IEEE Trans. Antennas Propag.*, vol. 51, no. 4, pp. 898–900, Apr. 2003.
- [20] Z. Qiang, "Simple structure high selectivity dual-band filtering antenna," in *Proc. 8th Int. Symp. Comput. Intell. Design (ISCID)*, Hangzhou, China, Dec. 2015, pp. 561–598.
- [21] C. Y. Hsieh, C. H. Wu, and T. G. Ma, "A compact dual-band filtering patch antenna using step impedance resonators," *IEEE Antennas Wireless Propag. Lett.*, vol. 14, pp. 1056–1059, 2015.
- [22] Y. Zhang, X. Y. Zhang, L.-H. Ye, and Y.-M. Pan, "Dual-band base station array using filtering antenna elements for mutual coupling suppression," *IEEE Trans. Antennas Propag.*, vol. 64, no. 8, pp. 3423–3430, Aug. 2016.
- [23] C.-X. Mao, S. Gao, Y. Wang, Q. Luo, and Q.-X. Chu, "A shared-aperture dual-band dual-polarized filtering-antenna-array with improved frequency response," *IEEE Trans. Antennas Propag.*, vol. 65, no. 4, pp. 1836–1844, Apr. 2017.
- [24] X. Y. Zhang, Y. Zhang, Y.-M. Pan, and W. Duan, "Low-profile dual-band filtering patch antenna and its application to LTE MIMO system," *IEEE Trans. Antennas Propag.*, vol. 65, no. 1, pp. 103–113, Jan. 2017.
- [25] K.-F. Tong, K.-M. Luk, K.-F. Lee, and R. Q. Lee, "A broad-band U-slot rectangular patch antenna on a microwave substrate," *IEEE Trans. Antennas Propag.*, vol. 48, no. 6, pp. 954–960, Jun. 2000.
- [26] C. X. Mao et al., "Dual-band patch antenna with filtering performance and harmonic suppression," *IEEE Trans. Antennas Propag.*, vol. 64, no. 9, pp. 4074–4077, Sep. 2016.
- [27] Y.-J. Lee, J.-H. Tarnag, and S.-H. Chung, "A filtering diplexing antenna for dual-band operation with similar radiation patterns and low cross-polarization levels," *IEEE Antennas Wireless Propag. Lett.*, vol. 16, pp. 58–61, 2017.
- [28] X. Y. Zhang, J.-X. Chen, Q. Xue, and S.-M. Li, "Dual-band bandpass filters using stub-loaded resonators," *IEEE Microw. Wireless Compon. Lett.*, vol. 17, no. 8, pp. 583–585, Aug. 2007.



CHUN-XU MAO was born in Hezhou, China. He received the M.S. degree in RF and microwave engineering from the South China University of Technology in 2013 and the Ph.D. degree from the University of Kent, U.K., in 2017. He is currently with the Computational Electromagnetics and Antennas Research Laboratory, Department of Electrical Engineering, Pennsylvania State University, USA, as a Post-Doctoral Research Associate. His research interests include filtering

antenna integration, UWB antenna, circularly-polarized satellite antenna array, multiband synthetic aperture radar antenna array, multifunctional RF frontend, and wearable antenna.

He has authored or co-authored over 30 papers in peer-reviewed international journals and conference proceedings. He received the Outstanding Master Thesis Award of Guangdong Province, China, in 2014. He also serves as a Reviewer for several journals, including the *IEEE TRANSACTIONS ON ANTENNAS AND PROPAGATION*, the *IEEE ACCESS*, *IEEE ANTENNAS AND WIRELESS PROPAGATION LETTERS*, the *IET Microwaves, Antennas & Propagation*.

STEVEN (SHICHANG) GAO (M'01–SM'16) is currently a Professor and the Chair of RF and Microwave Engineering, University of Kent, U.K. He has authored two books including *Space Antenna Handbook* (Wiley, 2012), and *Circularly Polarized Antennas* (IEEE–Wiley, 2014), over 200 papers, and several patents. His research covers smart antennas, phased arrays, MIMO, satellite antennas, RF/microwave/mm-wave circuits, satellite communications, UWB radars, synthetic-aperture radars, and mobile communications. He is an IEEE AP-S Distinguished Lecturer, an Associate Editor of the *IEEE TRANSACTIONS ON ANTENNAS AND PROPAGATION*, an Associate Editor of *Radio Science* and the Editor-in-Chief for Wiley Book Series on *Microwave and Wireless Technologies*. He was the General Chair of LAPC 2013, and a Keynote Speaker or Invited Speaker at some international conferences, such as AES'2014 (China), IWAT'2014 (Sydney), SOMIRES'2013 (Japan), and APCAP'2014 (China).

YI WANG (M'09–SM'12) received the B.Sc. degree in physics and the M.Sc. degree in condensed matter physics from the University of Science and Technology, Beijing, China, in 1998 and 2001, respectively, and the Ph.D. degree in electronic and electrical engineering from The University of Birmingham, in 2005. In 2011, he became a Senior Lecturer at the University of Greenwich, U.K. His current research interests include millimeter-wave/terahertz devices for metrology, communications and sensors, microwave circuits based on multi-port filtering networks, and antennas.

YING LIU (M'09–SM'16) received the M.S. and Ph.D. degrees in electromagnetics from Xidian University, Xi'an, China, in 2001 and 2004, respectively. From 2006 to 2007, she was a Post-Doctoral Researcher with Hanyang University, Seoul, South Korea. She is currently a Full Professor with the National Key Laboratory of Science and Technology on Antennas and Microwaves, Xidian University. She has authored or co-authored over 100 refereed journal papers. Her research interests include antenna theory and technology, prediction, and control of antenna RCS. She is a Senior Member of the Chinese Institute of Electronics. She was a recipient of the New Century Excellent Talents in University at the Ministry of Education, China, in 2011.

XUE-XIA YANG (S'98–A'01–M'02–SM'17) received the B.S. and M.S. degrees from Lanzhou University, Lanzhou, China, in 1991 and 1994, respectively, and the Ph.D. degree in electric engineering from Shanghai University, Shanghai, China, in 2001. From 1994 to 1998, she was a Teaching Assistant and a Lecturer with Lanzhou University. From 2001 to 2008, she was a Lecturer and an Associate Professor with Shanghai University, where she is currently a Professor and the Head of the Antennas and Microwave R&D Center. She is a member of the Committee of Antenna Society, China Electronics Institute, and a Senior Member of the China Electronics Institute.

ZHI-QUN CHENG is currently with Hangzhou Dianzi University, Hangzhou, China.

YOU-LIN GENG is currently with Hangzhou Dianzi University, Hangzhou, China.

• • •